Sign inversion of magnetoresistance in space-charge limited organic devices

DOI:
10.1103/PhysRevLett.103.066601

Document status and date:
Published: 01/01/2009

Document Version:
Publisher's PDF, also known as Version of Record (includes final page, issue and volume numbers)

Sign Inversion of Magnetoresistance in Space-Charge Limited Organic Devices

F. L. Bloom,* M. Kemerink, W. Wagemans, and B. Koopmans

Department of Applied Physics, Center for NanoMaterials, Eindhoven University of Technology, P.O. Box 513, 5600 MB Eindhoven, The Netherlands

(Received 26 March 2009; published 6 August 2009)

In this Letter, we explain the puzzling sign change of organic magnetoresistance in space-charge limited devices by device physics. We prove analytically and numerically that in the case of bipolar conduction with an Ohmic majority carrier and an injection limited minority carrier contact, a *decrease* in minority carrier mobility may give rise to an *increase* in the device current. It is shown that when the magnetic field acts to decrease the mobility of both carriers, a sign change in the magnetoconductivity as a function of applied bias may result. This behavior is in agreement with experimental observations.

DOI: 10.1103/PhysRevLett.103.066601 PACS numbers: 85.30.De, 72.80.Le, 73.43.Qt

Organic magnetoresistance (OMAR) is a magnetoresistance effect that has been observed in organic semiconductor devices without any magnetic materials [1,2]. At room temperature the effect can cause a large (>10%) magnetoconductance (MC), the relative change in conductance due to a magnetic field, at relatively low magnetic fields (~10 mT) [2]. These properties, combined with the chemical tunability and ease of processing of organic semiconductor materials, may make OMAR interesting for use in large area magnetic field sensing arrays.

So far, several mechanisms to explain OMAR have been proposed. All these mechanisms rely on random hyperfine fields inducing spin mixing, which an external magnetic field acts to decrease. This spin mixing can change the spin correlation between two-carrier states such as excitons and bipolarons or their precursor pairs, thus changing the singlet-triplet nature of these states. There are several mechanisms suggested on how this change in spin mixing can cause a change in current: it could change the recombination rate [3,4], alter the process of triplet-exciton polaron quenching [5,6], change dissociation of triplet-excitons by polarons [4] and electrodes [5,6], and finally the spin mixing could alter the process of bipolaron formation [7,8].

A crucial and puzzling property of OMAR is that the sign of the MC can depend on device thickness [5] as well as on operating conditions such as voltage [9–11] and temperature [9,12]. Several groups have studied these sign changes, motivated by the notion that further understanding them may provide an essential key towards resolving the microscopic origin of OMAR. Different explanations for the sign change have been reported [3,4,6,10,11], and generally it has been thought that different signs of OMAR correspond to differences in the microscopic mechanism at different device operating conditions.

In this Letter, we show that for bipolar devices operating under space-charge limited current (SCLC) conditions, an OMAR mechanism that causes magnetic contrast to both the hole and electron mobilities of the *same* sign will cause a sign change in the MC as a function of applied bias. This sign change occurs at the transition between the unipolar (small electrical bias) and the bipolar (large bias) regime and is shown to be a natural consequence of the device physics. More specifically, it will be shown how a *decrease* in the minority charge carrier mobility can lead to an *increase* in the total current. Although never noticed before, such a behavior should be more general for SCLC devices with one Ohmic and one current-limiting contact, potentially having applications well beyond OMAR in organic devices.

Sign changes in OMAR have been previously observed when the device changes from unipolar to bipolar transport as a function of increasing voltage [10,11,13]. Here we examine a case where the majority carrier injection is Ohmic and the minority carrier injection is injection limited. This is a common situation for bipolar devices at lower voltages, where the device is not yet fully bipolar [10,13]. In this case the transition from unipolar to bipolar behavior is a result of the electric field at the minority carrier contact becoming large enough that minority charges start to be injected and the device becomes slightly bipolar. At this point, the electric field throughout the device is still entirely determined by the majority carriers since the minority charge carrier density is low. As a consequence, the electrical field at the minority charge carrier contact is still insensitive to the density and mobility of the minority carriers, causing this contact to act like a constant current source. The consequences of this effect are schematically illustrated in Figs. 1(c)–1(e), where the mobility (μ) is represented by the arrows and the LUMO (HOMO) is the lowest (highest) molecular orbital. Let us assume that by applying a magnetic field the minority charge carrier mobility decreases. Then the density of minority charges increases because the injected current in the minority channel is constant [Figs. 1(d) and 1(e)]. The increase in the minority carrier density further compensates the Coulomb repulsion between the majority charges, causing the density of the majority charges to increase. Since the more mobile majority carriers carry the bulk of the current, an increase in their density increases the device

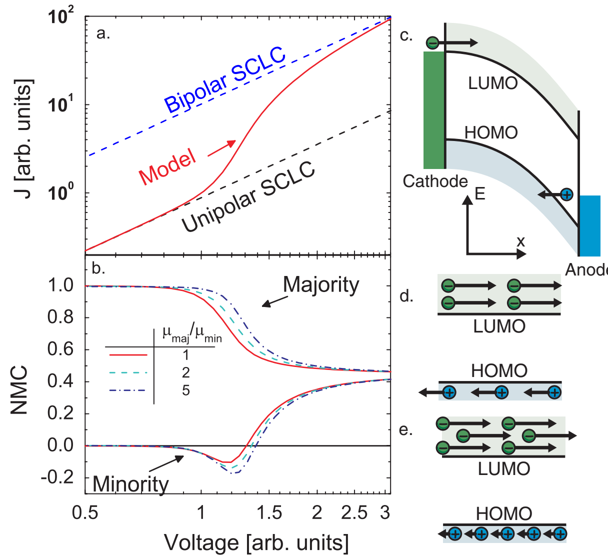

FIG. 1 (color online). (a) The analytically determined $J(V)$ with $\frac{\mu_{\rm maj}}{\mu_{\rm min}} = 2$, represented by "Model" (solid red line). The upper and lower limit of the current is given by bipolar SCLC (dashed blue line) and unipolar SCLC (dashed black line), respectively. (b) The analytically determined NMC versus voltage using different ratios of $\frac{\mu_{\rm maj}}{\mu_{\rm min}}$ in the case of a magnetomobility in the majority or minority channel. For all calculations $\frac{\mu_{\rm min}}{\mu_r} = 40$. (c) Schematic band diagram of the modeled device. The device has an Ohmic electron (majority carrier) contact and injection limited hole (minority carrier) contact. (d), (e) Diagrams showing the effect on the charge concentrations of the hole and electron channel as hole mobility is decreased (μ is represented by the length of the arrows).

current. Thus, the current can respond *oppositely* to a change in minority carrier mobility. As such, the minority channel acts as an internal gate that carries little current but significantly affects the charge density in the current carrying majority channel.

In order to understand the effect in a more quantitative way, we follow the analytical device model of SCLC as introduced by Parmenter and Ruppel [14]. Their treatment leads to the well-known relationships for unipolar and bipolar SCLC. In order to treat the intermediate case between unipolar and bipolar SCLC, it is required to include a concrete functional dependence for the minority charge carrier injection not outlined in [14] or [15].

To derive the relationships for unipolar and bipolar SCLC, Parmenter and Ruppel solved the coupled drift, Poisson, and current continuity equations [14]. We follow their solution of these equations but use specific boundary conditions: an Ohmic majority carrier (electron) contact at the cathode and an injection limited minority carrier (hole) contact at the anode (a detailed description is provided in the supplementary information [16]). We note that the choice of the electron as majority carriers is arbitrary, and the same physics will hold if holes are the majority carriers. In addition, we must explicitly model the hole current at the anode J_{a_h}, as a function of the electric field at the anode E_a. We found the general behavior, which we report on later, is qualitatively independent of the type of injection model we choose, and both phenomenological models with a certain onset electric field and more realistic injection models work well. Here we chose a phenomenological function which reproduces the experimentally observed current voltage [$J(V)$] behavior relatively well: $J_{a_h} = J_0(\exp[\frac{E_a}{E_0}] - 1)$, where E_0 determines how sharp the onset of the electron current is, and J_0 is a constant prefactor. In all of our modeling we used weak recombination where the recombination mobility μ_r was modeled using Langevin-type recombination given by $\mu_r = L(\mu_e + \mu_h)$, where μ_e and μ_h are the respective electron and hole mobilities, and $L \ll 1$ is a prefactor determining the strength of recombination.

Figure 1(a) (solid red line) shows the modeled current density $J_{\rm mod}$ as a function of voltage. We observe that at low voltage $J_{\rm mod}(V)$ can be described by unipolar SCLC (black dashed line). When the voltage becomes large enough the injection limited anode begins to inject holes resulting in the current becoming larger than unipolar SCLC, similar to what we observed experimentally [10]. At higher voltages, $J_{\rm mod}(V)$ converges to bipolar SCLC (blue dashed line) since the contact ceases to be injection limited due to the large E_a.

To determine how a magnetic field effect on the mobility (magnetomobility) affects the overall device current we calculated $J_{\rm mod}$ with and without a magnetic field. The magnetic field is assumed to cause a voltage independent change of the mobility. From this we determined a "normalized MC" (NMC_i), which is defined as the relative change in the total current due to a relative change in mobility of a single charge carrier $\frac{\Delta J}{J} / \frac{\Delta \mu_i}{\mu_i}$, where $i =$ min or maj indicating the minority and majority carriers, respectively [16]. At the unipolar low voltage limit, it is obvious that $\text{NMC}_{\rm maj} = 1$ and $\text{NMC}_{\rm min} = 0$ [Fig. 1(b)]. At high voltage the charge transport converges to bipolar SCLC, which results in a $\text{NMC}_{\rm maj}$ and $\text{NMC}_{\rm min}$ of 1/2 [16]. In the intermediate voltage regime, when there is a magnetomobility in the minority channel, we see very interesting behavior. Initially, at the beginning of minority charge carrier injection, the $\text{NMC}_{\rm min}$ is negative; therefore, increasing $\mu_{\rm min}$ results in a *decrease* in J for the reason outlined in Figs. 1(c)–1(e). At high voltages where the anode is no longer injection limited, the NMC converges to the expected bipolar behavior. In between we see that there is a local minimum in the $\text{NMC}_{\rm min}(V)$ followed by a sign change as a result of this transition away from injection limited behavior to bipolar SCLC. We also observe that increasing the mobility ratio $\frac{\mu_{\rm maj}}{\mu_{\rm min}}$ results in the $\text{NMC}_{\rm min}$ becoming more negative. $\Delta\mu_{\rm min}$ acts to change the current in the majority channel by increasing the majority carrier density, while the current in the injection limited minority channel remains constant. Therefore, the larger $\frac{\mu_{\rm maj}}{\mu_{\rm min}}$, the more of the current is carried by the majority channel and the more negative $\text{NMC}_{\rm min}$.

To model more realistic conditions, we solved the drift and diffusion equations numerically using the principles laid out by Malliaras and Scott [17]. We extended their approach to include trapping in the majority charge carrier (electron) channel (a detailed description is provided in the supplementary information [16]). The energetic distribution of traps below the LUMO was approximated with an exponential density of states with a width of $5k_BT$, where k_B is Boltzmann's constant and T is the temperature. The trapping time was set to 10 ms, while the detrapping was calculated according to the principles of detailed balance. This results in trap filling according to Fermi-Dirac statistics.

We modeled the device using an Ohmic contact for the cathode, modeled by Boltzmann injection with a barrier height of 0.1 eV, and an injection limited anode, modeled by thermionic emission with a barrier height of 0.8 eV. Langevin recombination was used with $L = 0.01$. Figure 2(a) shows the numerically calculated $J(V)$. Here we observe, like in the analytical model, that at low voltages the $J(V)$ follows a unipolar power law behavior [black dashed line Fig. 2(a), calculated with Ohmic cathode and a blocking anode) with a power of $n > 2$ due to trapping [18]. We observe a deviation from the power law behavior once minority charge carrier injection begins, like observed experimentally [10,13]. At high voltage the $J(V)$ behavior saturates to bipolar behavior [blue dashed line Fig. 2(a), calculated with two Ohmic contacts].

When there is a magnetomobility in the minority channel, the onset of MC occurs at the onset of minority charge injection and the $\mathrm{NMC}_{\mathrm{min}}$ is negative at this onset [red circles Fig. 2(b)]. As the voltage increases there is a local minimum in the $\mathrm{NMC}_{\mathrm{min}}(V)$. After this minimum the $\mathrm{NMC}_{\mathrm{min}}$ then increases and eventually changes sign. This is the same qualitative $\mathrm{NMC}_{\mathrm{min}}(V)$ behavior as in the analytical model. If there are magnetomobilities in both the minority and majority channels, which is possible in the bipolaron model for OMAR [7,8], we see that the model would predict two sign changes [dashed lines in Fig. 2(b)]. In single carrier devices it has been observed that OMAR has a stronger effect on the minority channel [11,19], so the case where $|\frac{\Delta\mu_{\mathrm{maj}}}{\mu_{\mathrm{maj}}}| < |\frac{\Delta\mu_{\mathrm{min}}}{\mu_{\mathrm{min}}}|$ would be more realistic.

One major difference between the numerical and analytical models is that the negative $\mathrm{NMC}_{\mathrm{min}}$ is much larger in the numerical model. This is due to the presence of majority traps. By removing the traps from the majority channel, the negative $\mathrm{NMC}_{\mathrm{min}}$ becomes much smaller (Fig. 3). The $\mathrm{NMC}_{\mathrm{min}}$ results from changing the Coulomb repulsion in the majority channel by indirectly modifying the minority carrier density by altering the minority charge carrier mobility. Therefore, it seems reasonable that increasing the Coulomb repulsion by adding traps to the majority channel increases the strength of the negative $\mathrm{NMC}_{\mathrm{min}}$. If we look at how changing the $\frac{\mu_{\mathrm{maj}}}{\mu_{\mathrm{min}}}$ ratio affects $\mathrm{NMC}_{\mathrm{min}}$, it seems that the enhancement of the

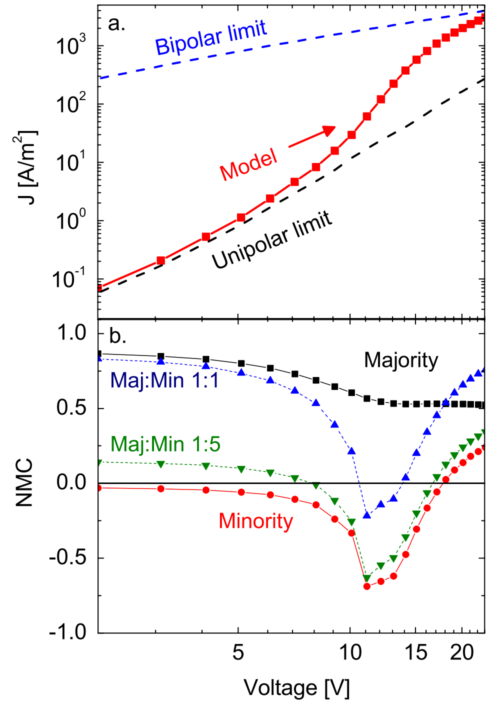

FIG. 2 (color online). (a) The numerically determined $J(V)$ of a device with traps in the majority channel and $\frac{\mu_{\mathrm{maj}}}{\mu_{\mathrm{min}}} = 2$, represented by "Model" (red line). The upper and lower limit of the current is given by the "bipolar limit" (dashed blue line) and "unipolar limit" (dashed black), respectively. (b) The NMC versus voltage in the case of magnetomobility in the majority (black squares) and minority (red circles) channels, respectively, as well as for both channels combined, with $\frac{\Delta\mu_{\mathrm{maj}}}{\mu_{\mathrm{maj}}} = \frac{\Delta\mu_{\mathrm{min}}}{\mu_{\mathrm{min}}}$ (blue up-pointing triangles) and $5\frac{\Delta\mu_{\mathrm{maj}}}{\mu_{\mathrm{maj}}} = \frac{\Delta\mu_{\mathrm{min}}}{\mu_{\mathrm{min}}}$ (green down-pointing triangles), normalized to $\frac{\Delta\mu_{\mathrm{min}}}{\mu_{\mathrm{min}}}$.

negative $\mathrm{NMC}_{\mathrm{min}}$ due to trapping dominates the effect of the $\frac{\mu_{\mathrm{maj}}}{\mu_{\mathrm{min}}}$ ratio (Fig. 3, solid symbols). However, in the case without traps, increasing the $\frac{\mu_{\mathrm{maj}}}{\mu_{\mathrm{min}}}$ ratio makes $\mathrm{NMC}_{\mathrm{min}}$ more negative (Fig. 3, open symbols), like in the analytical model.

The fact that the change in current reacts oppositely to a magnetomobility in the minority channel may be important in resolving apparent inconsistencies between experiments and the bipolaron model. The bipolaron model predicts both a positive magnetomobility ($\frac{d\mu}{d|B|} > 0$) and negative magnetomobility ($\frac{d\mu}{d|B|} < 0$) [7,8], where B is the applied magnetic field. According to this model the maximum magnitude of the negative magnetomobility is larger than that of the positive magnetomobility. However, the largest MCs that have been observed are positive, which is inconsistent with the bipolaron model unless the current can react oppositely to the change in the mobility. By showing this with our models we can resolve this inconsistency.

More strongly, by using these models all the sign change behavior in literature can be explained when the magnetomobility is negative. Therefore, there is no need to *ad hoc* assign different signs of magnetomobilities to different

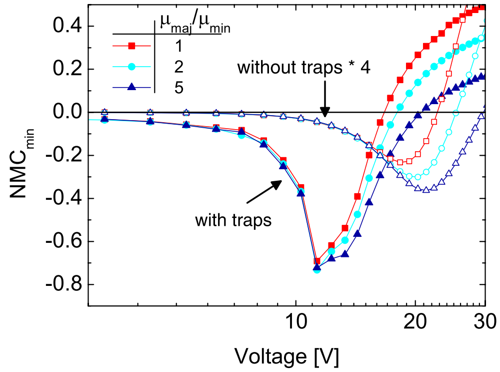

FIG. 3 (color online). NMC_{min} versus voltage for the case with (solid symbols) and without (open symbols) traps in the majority channel for different ratios of $\frac{\mu_{maj}}{\mu_{min}}$. The magnitude of the NMC_{min} for the calculations without trapping has been multiplied by a factor of 4 to make these curves more visible.

carriers or mechanisms. Two types of sign change behavior have been observed in literature. In one case, the MC changes from negative to positive with increasing voltage, which occurs at the transition between unipolar and bipolar behavior [10,11,13]. The resulting line shape is a superposition of two contributions of opposite sign and different field widths, which may be a result of separate magnetic field effects on electrons and holes [10]. In the other case, the sign change occurs at high voltage and goes from positive MC to negative MC with increasing voltage, with a line shape that remains unchanged (Fig. 4 in Ref. [9]). This result is consistent with the high voltage sign we observe in NMC_{min} in our models, which results from the minority contact becoming less injection limited as the voltage increases. If in our models negative magnetomobility for both carriers is assumed, the predicted signs of MC for the different transport regimes are exactly the same as experimentally observed.

Of course, observing both sign changes within a single device would provide conclusive experimental evidence that these models are applicable. However, observing the two sign changes in one device may be difficult since, as seen in Fig. 2, the numerical modeling shows these sign changes occur at currents that are separated by several orders of magnitude, making it difficult to observe both sign changes. However, it is common to observe a peak in the MC(V) [6,11,13,20], like we observe in the models (if one considers a negative magnetomobility) as the device becomes less injection limited. Moreover, we also observed that the second sign change is moved to higher voltages or even completely eliminated for a $J_{a_h}(E_a)$ dependence that does not allow the device to fully saturate to bipolar SCLC at high voltages.

In conclusion, we have shown phenomenologically, analytically, and numerically that by assigning a magnetic contrast of the *same* sign to the mobilities of electrons and holes one can explain both the sign change in the MC as well as its magnitude. This provides strong evidence that the OMAR is an effect on the carrier mobility. The fact that the MC(V) behavior may be so strongly dependent on device physics and not on the microscopic mechanism highlights that the microscopic mechanism of OMAR need not change as a function of voltage. Finally, this device physics is not limited to OMAR; it should also be applicable to any SCLC device with one Ohmic contact and one injection limited contact in which mobilities can be externally influenced.

This work was supported by the Dutch Technology Foundation (STW) via the NWO VICI-Grant "Spin Engineering in Molecular Devices."

*f.l.bloom@tue.nl

[1] J. Kalinowsky, J. Szmytkowski, and W. Stampor, Chem. Phys. Lett. **378**, 380 (2003).
[2] T.L. Francis, Ö. Mermer, G. Veerarghavan, and M. Wohlgenannt, New J. Phys. **6**, 185 (2004).
[3] J.D. Bergeson, V.N. Prigodin, D.M. Lincoln, and A.J. Epstein, Phys. Rev. Lett. **100**, 067201 (2008).
[4] B. Hu and Y. Wu, Nature Mater. **6**, 985 (2007).
[5] P. Desai, P. Shakya, T. Kreouzis, W.P. Gillin, N.A. Morley, and M.R.J. Gibbs, Phys. Rev. B **75**, 094423 (2007).
[6] P. Desai, P. Shakya, T. Kreouzis, and W.P. Gillin, J. Appl. Phys. **102**, 073710 (2007).
[7] P.A. Bobbert, T.D. Nguyen, F.W.A. vanOost, B. Koopmans, and M. Wohlgenannt, Phys. Rev. Lett. **99**, 216801 (2007).
[8] W. Wagemans, F.L. Bloom, P.A. Bobbert, M. Wohlgenannt, and B. Koopmans, J. Appl. Phys. **103**, 07F303 (2008).
[9] Ö. Mermer, G. Veeraraghavan, T.L. Francis, Y. Sheng, D.T. Nguyen, M. Wohlgenannt, A. Köhler, M.K. Al-Suti, and M.S. Khan, Phys. Rev. B **72**, 205202 (2005).
[10] F.L. Bloom, W. Wagemans, M. Kemerink, and B. Koopmans, Phys. Rev. Lett. **99**, 257201 (2007).
[11] F.J. Wang, H. Bässler, and Z. Valy Vardeny, Phys. Rev. Lett. **101**, 236805 (2008).
[12] F.L. Bloom, W. Wagemans, and B. Koopmans, J. Appl. Phys. **103**, 07F320 (2008).
[13] F.L. Bloom, W. Wagemans, M. Kemerink, and B. Koopmans, Appl. Phys. Lett. **93**, 263302 (2008).
[14] R.H. Parmenter and W. Ruppel, J. Appl. Phys. **30**, 1548 (1959).
[15] B.G. Martin, J. Appl. Phys. **75**, 4539 (1994).
[16] See EPAPS Document No. E-PRLTAO-103-009934 for supplementary information. For more information on EPAPS, see http://www.aip.org/pubservs/epaps.html.
[17] G.G. Malliaras and J.C. Scott, J. Appl. Phys. **83**, 5399 (1998).
[18] P.W.M. Blom, M.J.M. de Jong, and J.J.M. Vleggaar, Appl. Phys. Lett. **68**, 3308 (1996).
[19] T.D. Nguyen, J. Rybicki, Y. Sheng, and M. Wohlgenannt, Phys. Rev. B **77**, 035210 (2008).
[20] U. Niedermeier, M. Vieth, R. Pätzold, W. Sarfert, and H. von Seggern, Appl. Phys. Lett. **92**, 193309 (2008).